Coupling of a subsurface drainage model with a soil reservoir model to simulate drainage discharge and drain flow start

Hocine Henine, Cédric Chaumont, Alexis Jeantet, Samy Chelil, Claire Lauvernet, Julien Tournebize

Coupling of a subsurface drainage model with a soil reservoir model to simulate drainage discharge and drain flow start

Authors:

Hocine Henine[1,*], Alexis Jeantet[1], Cédric Chaumont[1], Samy Chelil[1], Claire Lauvernet[2], Julien Tournebize[1]

[1] INRAE, University of Paris-Saclay, UR HYCAR, Jouy-en-Josas - Antony

[2] INRAE, UR RiverLy, Lyon

[*] Corresponding Author:

Hocine Henine, Hocine.henine@inrae.fr. INRAE, University of Paris-Saclay, UR HYCAR, Jouy-en-Josas - Antony

Abstract

The environmental impact of subsurface drainage and agricultural activities has been widely studied in the literature. Agricultural subsurface drainage modifies the hydrological behavior and accelerates the transfer of pollutants of agricultural origin into surface water during the drain flow period, which is often limited to winter. The main objective of this study is to present a modeling approach allowing an accurate modeling of subsurface drainage discharge and prediction of drain flow start times, by integrating a new conceptual soil reservoir, managing the water flow in the unsaturated zone, to the SIDRA model. A comparison of the model results with field measurements of drainage discharge at the "La Jaillière" site (France) shows that such a model can efficiently simulate drainage discharge (KGE values > 0.75) and predict, with good accuracy, the drain flow start time (with a median value of 5 days

and a standard deviation of 10 days). The split simple test conducted for the model calibration and validation shows that the model is temporally robust. A sensitivity analysis conducted using the Sobol method on the five model parameters reveals that the drainage discharge simulation is mainly sensitive to the hydraulic conductivity and drainable porosity parameters. On the other hand, the date delimiting drain flow start is sensitive to the soil reservoir parameters. The model's ability to accurately predict the start of drain flow serves to avoid the application of farm inputs (pesticides or fertilizers) during this critical period in order to limit their transfer to surface waters.

Keywords

Subsurface drainage, modeling, drain flow start, tile-drained field.

1 Introduction

Land improvements contribute to agricultural intensification, which in turn leads to greater crop production from the same parcel. Among such improvements, subsurface drainage (SD) is practiced to remove the temporary excess water from the root zone for purposes of: better aeration, higher temperatures and enhanced workability of the soil in humid regions. In arid and semi-arid regions, the primary function of SD is to prevent irrigation-induced waterlogging and soil salinization (Ritzema, 1994). In Europe, SD is mainly devoted to preventing waterlogging in specific hydromorphic soils; this practice is principally employed in Northern Europe, on over 50% of arable land (from the Netherlands to Finland), vs. approximately 10-20% for other European countries. In France, out of the 27 million hectares of arable land, more than 10% are subsurface drained (AGRESTE, 2010; Vincent, 2020). Subsurface drainage was established in France later than in other European countries, i.e. during the 1980's; it was promoted by European and national-level subsidies until 1992, when current water laws began limiting the extent of additional SD practices.

Agricultural SD introduces significant modifications to the hydrological behavior and results in nutrient and fertilizer losses from farmland to surface water (Blann et al., 2009; Gramlich et al., 2018). During

the drainage period, the application of mobile pesticides or fertilizers before a heavy rainfall increases their losses toward the SD outlet and the water surface (Boithias et al., 2014; Nolan et al., 2008). The temporary functioning of SD systems, mainly during the wet season, allows adapting the timing of when to apply farm inputs to reduce losses, e.g. increasing the interval between an application and the first drain flow of the drainage season (Brown and van Beinum, 2009; Trajanov et al., 2015; Wilson et al., 2020). An accurate prediction of this first drain flow is key to optimizing the timing of farm input application, thereby decreasing the risk of their transfer toward the water surface (L Jones et al., 2000; Lewan et al., 2009; Nolan et al., 2008; Trajanov et al., 2015; Willkommen et al., 2019).

The behavior of SD systems can be simulated by means of a physical or hydraulic approach. The physical approach is based on the numerical resolution of a physical law, such as the 3D Richards equation. Several physically-based models propose specific conditions for considering the presence of SD, e.g. in HYDRUS, SOIL, CATHY, DDM and 2D-DPERM (Al Jabri and Youngs, 2015; Boivin et al., 2006; Dusek and Vogel, 2014; Gärdenäs et al., 2006; Gatel et al., 2019; Gerke et al., 2013; Mehdinejadiani and Fathi, 2020; Shokri and Bardsley, 2016). The hydraulic-based approach merely considers the flow in a saturated zone and proposes a simplified equation, derived from both the Boussinesq equation (1904) and Forchheimer's hypothesis (Guyon, 1963; Henine et al., 2014; Van Schilfgaarde, 1963), to calculate drainage discharge as a function of water table height at mid-drain. The Hooghoudt drainage equation (Hooghoudt, 1940), which relates steady-state drainage discharge to the water table height at mid-drain, is the most widely used approach in SD modeling. When the water table rises to the soil surface for relatively long periods, drainage discharge is computed using the Kirkham equation (Kirkham, 1949) for ponded water. The approach proposed by Moriasi et al. (2013) couples Kirkham's simplified equations with the Hooghoudt equation (Hooghoudt, 1940; Kirkham, 1949) to examine long time series of subsurface drained experimental facilities; this approach offers the advantage of simulating both small and peak flow discharges. The Kirkham and Hooghoudt equations were integrated into the DRAINMOD model (Skaggs, 1980). The models MACRO (Jarvis and Larsbo, 2012), SWAP (Kroes et al., 2008) and many others adopt different equations (such as Hooghoudt, Kirkham's

and Ernst equations) or use seepage potential theory by considering the drain as a sink term to take into account subsurface drainage (Qi and Qi, 2016; Youngs, 1980). Guyon (1963) and Lesaffre and Zimmer (1987) developed the SIDRA (*SImulation of DRAinage*) model to simulate drainage discharge during the drainage season, based on the numerical integration of Boussinesq's equation between the drain and mid-drain. In relying on this same Boussinesq equation, Stillman et al. (2006) proposed another semi-analytical equation to simulate drainage discharge. These various simplified approaches have been incorporated into several distributed hydrological and GIS-based models for the purpose of integrating the SD function, e.g. SWAT (Moriasi et al., 2012), HYPE (Lindstrom et al., 2010) and ADAPT (Gowda et al., 2012).

The models derived from the Boussinesq equation are well adapted to simulate the hydrological behavior of SD, including peak flow prediction (Lesaffre and Zimmer, 1988). However, they become less suitable once the goal turns to predicting the environmental impact of agricultural SD. It is necessary to take into account the hydrodynamic behavior of the unsaturated zone as well as the plant growth impact on water table recharge and, hence, on drainage discharge. In this context, a coupling of the behavior in both saturated and unsaturated zones within a simple hydraulic approach for SD behavior modeling would offer a better understanding of the underlying environmental impacts. A coupled agronomic-hydrological model, namely STICS-SIDRA (Tournebize et al., 2004), was developed to manage the saturated and unsaturated zones; however, this crop model requires numerous parameters only available in certain fields of experimental research.

This paper integrates a new conceptual soil reservoir module into the hydraulic-based SIDRA model in order to predict both drainage discharge and drain flow starts. The conceptual module simulates water transfer in the unsaturated zone and calculates the recharge of the perched water table, which then serves as SIDRA input data. To simplify the model as much as possible, this conceptualization needs to be easily implemented and should improve both the prediction of drainage discharge and drain flow start every hydrological year.

The proposed model has been calibrated and validated using the dataset collected from two experimental drained plots located at the “La Jaillière” site (western France). The model's performance evaluation criterion is based on a comparison between simulated and observed drainage discharge, as well as on the drainage season start date. A global sensitivity analysis has also been conducted to study the influence of input parameters on model performance.

2 Experimental set-up

2.1 Experimental study sites

The "La Jaillière" experimental site (Figure 1) is located in western France's Loire-Atlantique Department (47°27’ N, 0°57’ W); it has been managed by the Arvalis Institute (French agricultural institute) since 1987. The experiments and research work carried out here focus on several study objectives, in particular to achieve satisfactory control over both water quality and quantity of the SD system. Several experiments have been ongoing since its inception, thus providing a most valuable dataset covering nearly 30 years.

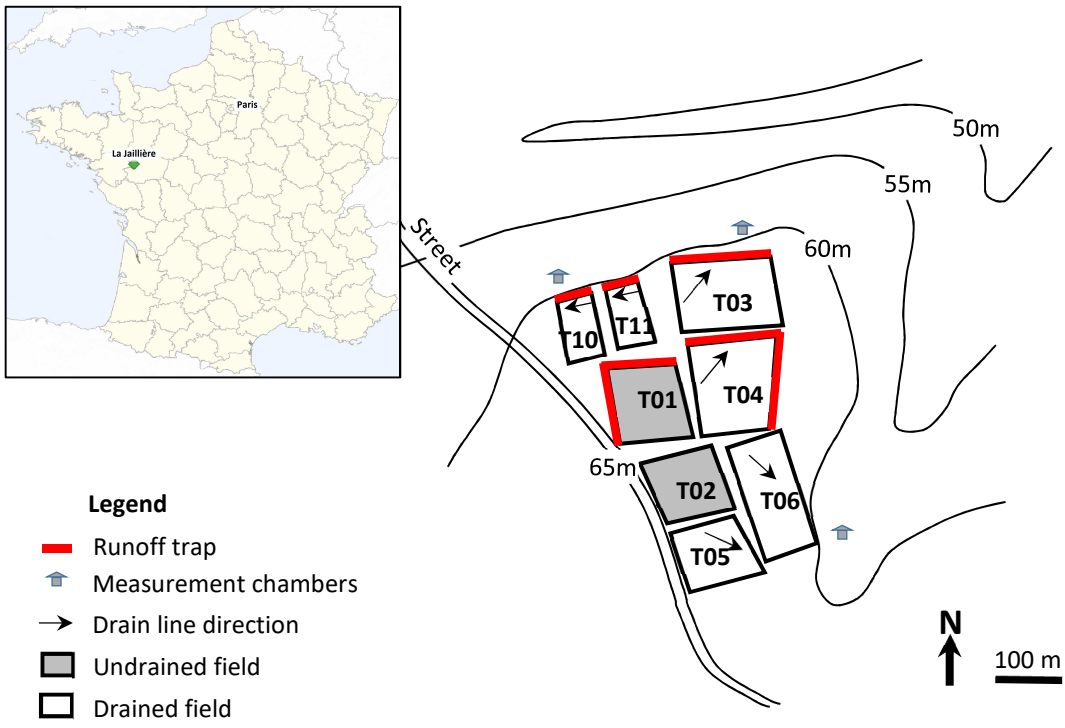

Figure 1: The "La Jaillière" experimental study site and its general location (Arvalis, Maine-et-Loire, France)

The climate in the study area is oceanic with a mean annual rainfall of 709 mm; the mean annual temperature is approximately 11°C. The mean potential evapotranspiration (PET) reaches 738 mm a year. The period of water budget deficit begins in April and continues until the end of September. Subsequent to this period, the excess net rainfall allows for a progressive saturation of the soil and the formation of a temporary perched water table, at which point the drain flow starts.

The soil at the La Jaillière site is a brown, hydromorphic stagnic luvisol (FAO 2006) developed on a low permeability, altered schist formation (Dairon et al., 2017). The soil surface layer (< 30 cm deep) consists of a sandy loam (16-22% clay), while the underlying layer, of variable thickness (from 30 to 90 cm), is richer in clay (> 30%, clayey-silty texture). The depth of the altered schist formation is highly variable within the studied plots, ranging from 0.6 to 1.2 m, and represents a natural obstacle to water infiltration. This impervious layer is responsible for temporary waterlogging through the formation of a perched water table. For each experimental plot (Table 1), the water holding capacity (see Section 3.1) was estimated from the textural soil analysis at a 0.8-m soil profile, by use of Rawls' linear regression equation (Rawls and Brakensiek, 1982).

Table 1: Characteristics of the experimental plot at the La Jaillière site: drainage design (depth and drain spacing), surface area, and Water Holding Capacity (WHC) calculated at a 0.8-m soil profile

Plot	Drain depth (m)	Drain spacing (m)	Surface area (ha)	WHC (mm)	Type of collected water
T01	-	-	0.83	97	Surface runoff
T02	-	-	0.90	96	-
T03	0.8-1.0	10	1.04	84	Surface runoff / Drainage
T04	0.8-1.0	10	1.08	104	Surface runoff / Drainage

T06	0.8-1.0	10	1.01	103	Drainage
T10	0.8-1.0	10	0.42	95	Surface runoff / Drainage
T11	0.8-1.0	10	0.42	99	Surface runoff / Drainage

128

129 To prevent soil waterlogging and improve crop growth during winter, an SD network was installed in
130 the 1980's (Table 1). Each experimental drained plot has been equipped with an individual drainage
131 network (10 m drain spacing, installed at a depth of 0.8 - 1 m), connected to a non-perforated collector
132 extending to the measurement chamber. For each field, the drainage discharge and surface runoff are
133 collected and measured separately. The surface runoff is collected using traps around each plot (Figure
134 1). The flow discharge is then measured hourly at each collector outlet using a V-notch weir. The water
135 level upstream of the weir, measured with an automatic pressure probe, is proportional to the flow
136 discharge.

137 Meteorological data are available at two stations (Trajanov et al., 2018). The former station from 1982
138 is located 1.4 km from the fields, while the new one (in operation since 2006) is located at the
139 experimental site.

140 2.2 Observation data

141 For purposes of model assessment, the dataset collected for experimental plots T03 (1.04 ha) and T04
142 (1.08 ha) is used to validate SIDRA-RU model. These datasets comprise hourly subsurface drainage
143 discharge (from 1994 to 2010) and surface runoff (from 1994 to 2004).

144 Since the meteorological data recorded at the study site contain many gaps, we have used the rainfall
145 and Potential EvapoTranspiration (PET) data from the SAFRAN meteorological reanalysis produced by
146 the Météo-France Agency (Vidal et al., 2010), defined on 8 km × 8 km grids at the national scale. While

147 these PET data can be considered as homogeneous on the 8 km × 8 km SAFRAN grid, the rainfall data
148 should display more local variation, which can exert a rather significant impact on modeling accuracy
149 of the two studied plots.

150 One of the mitigation solutions of pesticides losses from subsurface drained fields is to increase the
151 time interval (of several days) between their application and first drain flow (Brown and van Beinum,
152 2009; Trajanov et al., 2015). Thus, the SIDRA-RU model needs to be efficient and capable of accurately
153 predict drainage discharge and drain flow start. This accuracy depends on the method or criterion used
154 to set the drain flow start date. At the beginning of the drainage season, drain flow is often low and
155 quick; also, several days may pass without any drain flow at all. This specificity is difficult to reproduce
156 with acceptable accuracy by the models. To overcome the low flows that fail to indicate the actual
157 start of the drainage season, we have introduced herein a new method using two static thresholds
158 conditions: (1) the calculated cumulative drainage discharge must be greater than the initial threshold;
159 and (2) the additional cumulative drainage discharge within the 5 subsequent days must be greater
160 than the second threshold. Based on the experimental dataset, the first and second thresholds are set
161 to 2 and 2.5 mm, respectively.

162 From the drainage discharge measurement, we defined the drain flow start dates for each season. The
163 yearly cumulative values of meteorological data, drainage discharge and surface runoff plus the drain
164 flow start dates used in this study are listed in Table 2.

165 Table 2: Yearly cumulative values of meteorological data (PET, rainfall), drainage discharge (Qdrain)
166 and surface runoff, plus drain flow start dates on Plots T03 and T04. Values between parentheses (*)
167 represent the cumulative rainfall and PET over drain flow periods (Qdrain > 0)

Drainage seasons	**PET (*) (mm)**	**Rainfall (*) (mm)**	T03 plot			T04 plot		
			Qdrain (mm)	**Runoff (mm)**	**Drain flow start**	**Qdrain (mm)**	**Runoff (mm)**	**Drain flow start**

1994-1995	723 (586)	947 (787)	484	64	24-Oct	500	-	23-Sept
1995-1996	763 (334)	586 (414)	134	13	22-Dec	109	10	27-Dec
1996-1997	727 (117)	606 (286)	189	16	28-Nov	165	15	29-Nov
1997-1998	675 (162)	709 (399)	221	15	11-Dec	193	22	10-Dec
1998-1999	706 (342)	779 (610)	280	34	19-Oct	290	37	24-Nov
1999-2000	634(288)	945 (764)	438	34	19-Sept	382	57	19-Sept
2000-2001	644 (292)	1128 (990)	519	76	11-Oct	512	113	16-Oct
2001-2002	631 (110)	614 (260)	156	39	18-Oct	144	14	29-Dec
2002-2003	649 (164)	887 (566)	398	46	4-Sept	328	28	2-Nov
2003-2004	681 (246)	629 (427)	247	-	14-Nov	237	29	16-Nov
2004-2005	704 (66)	506 (85)	24	-	5-Jan	10	-	20-Jan
2005-2006	739 (131	594 (298)	122	-	4-Jan	121	-	4-Dec
2006-2007	677 (352)	1029 (778)	278	-	19-Oct	274	-	21-Oct
2007-2008	691 (279)	682 (464)	231	-	27-Nov	174	-	5-Jan
2008-2009	668 (247)	646 (353)	133	-	10-Nov	113	-	9-Dec
2009-2010	735 (231)	650 (423)	181	-	28-Nov	226	-	28-Nov
Mean	**690 (247)**	**746 (494)**	**252**	37	**10-Nov**	**236**	36	**23-Nov**
Standard deviation	40 (127)	184 (238)	141	22	-	140	32	-

Table 2 shows that the yearly drainage discharge correlates with the yearly rainfall. The PET shows a small inter-annual variation (with a mean value of 690 and a standard deviation of 40 mm). In the wet period (autumn and winters seasons), the PET demand is generally satisfied and the excess of rainfall (P-PET) causes drainage discharge (Qdrain) and surface runoff. Assuming that deep infiltration under the drainage network is negligible during the drain flow period, the average evapotranspiration (AET, computed as Rainfall - Qdrain - Surface Runoff) accounts for 86% of PET. However, in the dry period,

175 the PET demand is poorly satisfied and there occurs neither drain flow nor surface runoff. The yearly
176 average AET accounts for 67% of PET. The rainfall and drainage discharge dataset displays high
177 hydrological variability with respect to both dry (e.g. season 2004-05) and wet seasons (e.g. 2000-01).
178 Analysis of Table 2 suggests that the start of drainage season is highly variable from one season to
179 another. In average, the drainage season starts in mid-November, however, it can start early (in
180 September) or very late (in January). The drainage season 2004-2005 started later in January 5 and
181 presented a low cumulative drainage discharge (of 10 mm). Drain flow often starts earlier on plot T03
182 than on T04, despite their similarity during the intense drainage season. The low WHC value for plot
183 T03 (Table 1) allows filling the soil profile and generating a water table flow toward drains earlier on
184 the this plot, as compared to T04. From the data observed in Table 2, surface runoff accounts for 12%
185 and 10% of the total outflow of plots T04 and T03, respectively.

186 # 3 Model description

187 Drain flow occurs when the perched water table rises above the drains. The SIDRA model simulates
188 drainage discharge during the soil profile saturation period, defined as the Intensive Drainage Season
189 (IDS) by Lesaffre and Zimmer (1988). The new SIDRA-RU model presented herein allows SIDRA to
190 simulate SD discharges and hydrological behavior at the plot scale during a full hydrological year and
191 extending for several subsequent years. The proposed model has been based on three coupled
192 modules (Figure 2) managing the flow paths: in the soil surface, in the unsaturated zone, and in the
193 water table temporally perched above the drains. These three modules, integrated into the current
194 version of SIDRA-RU, are as follows:

195 1. Module 1: Estimation of net infiltration from climatic data, by integrating a more realistic
196 evapotranspiration algorithm that takes into account the potential evapotranspiration
197 rate (PET) and available soil water content in the soil reservoir S(t). The new value
198 calculated during this step is referred to as “corrected evapotranspiration” (or CET). Net
199 infiltration is equal to rainfall (P) minus corrected evapotranspiration (CET);

2. Module 2: Management of water transfer in the unsaturated zone, in order to calculate the net recharge into the drained water table, based on the conceptual reservoir approach. This module calculates net recharge as a function of the available soil water content in the soil reservoir S(t), relative to three distinct soil reservoir levels, namely minimum (S_{min}), intermediate (S_{inter}) and maximum (S_{max});
3. Module 3: Simulation of the SD discharge (Q) as a function of the mid-drain water table height above drain (H) by applying the SIDRA model (Lesaffre and Zimmer, 1988).

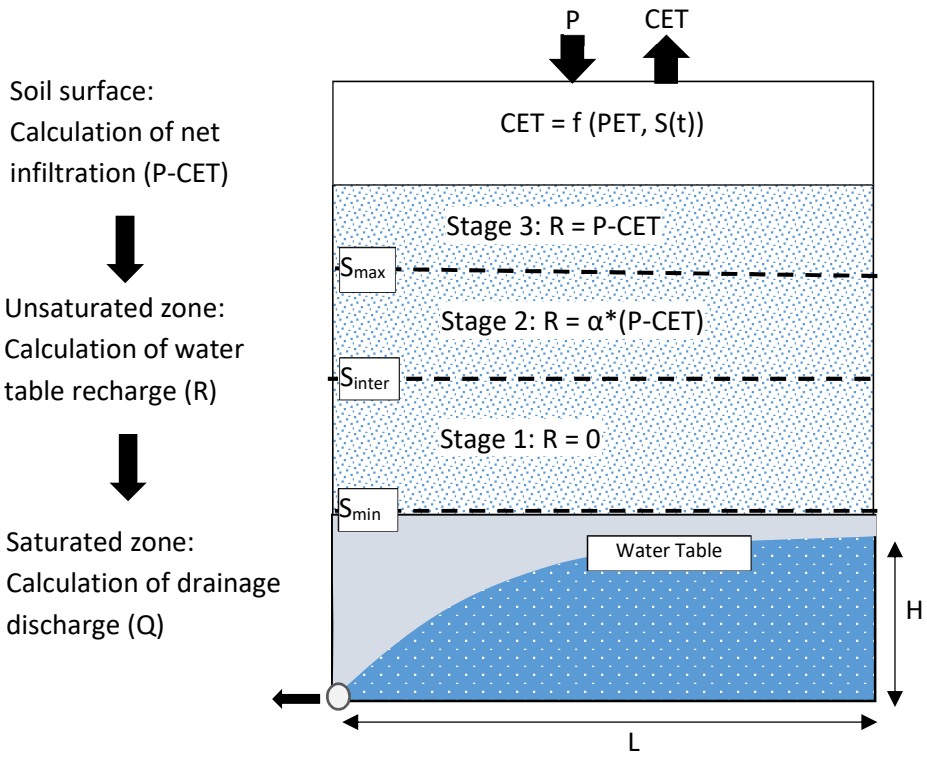

Figure 2: Diagram presenting the three SIDRA-RU modules, with P: rainfall [LT^{-1}], CET: corrected evapotranspiration [LT^{-1}]; S(t): actual water level in the soil reservoir [L]; S_{min}: minimum soil reservoir level (= 0 mm); S_{inter}: Intermediate soil reservoir level [L]; S_{max}: maximum soil reservoir level [L]; R(t): water table recharge [LT^{-1}]; L : distance between the drain and mid-drain [L]; H: mid-drain water table height above drain [L]; and Q: drainage discharge per unit area [$L^3T^{-1}L^{-2}$]. The dashed horizontal lines indicate the soil reservoir module levels. α: partition coefficient representing the part of net infiltration which recharges the water table during the stage 2.

3.1 Calculation of the corrected evapotranspiration

To estimate net rainfall infiltration, this module calculates a more realistic evapotranspiration value, referred to here as corrected evapotranspiration (CET). This CET depends on the potential evapotranspiration (PET), the available soil water content in the soil profile and the type of vegetation (Hansen, 1984; Kristensen and Jensen, 1975). Depending on the type of vegetation, CET is transformed into the maximum evapotranspiration rate (MET) by means of the crop coefficient, β. When the soil water content lies in the range of the extractable soil water (ESW), the CET/PET ratio is equal to β. This value represents the share of the WHC that allows plants to extract water from the soil without either water constraints or growth limitations (Hansen, 1984; Jacquart and Choisnel, 1995). Soil WHC represents the amount of water held by soil against gravity force that can be extracted either by evaporation or by root plant (Bordoloi et al., 2019). Under France's agro-climatic conditions, ESW varies from 0.4 to 0.6 of WHC, as a function of root depth (Jacquart and Choisnel, 1995). In this study, ESW has been set equal to 0.6 of WHC. This value defines the lower limit of soil water content in the soil profile, at which CET equals the maximum evapotranspiration rate (MET). When the soil water content in the soil profile lies below ESW, less water is available for root extraction; Eq. 1 proposes an exponential decrease of CET with water level in the soil reservoir S(t). To simplify the model parameterization and to take into account the non-uniformity of the soil water content in the soil profile, WHC has been approximated at the intermediate soil reservoir level S_{inter} of the conceptual soil reservoir model (Section 3.2 below). The module computes CET [L] as follows:

$$\begin{aligned} &\text{Case 1: If } (S(t) > 0.6 * \mathrm{S_{inter}}) && \mathrm{CET} = \mathrm{MET} = \beta * \mathrm{PET} \\ &\text{Case 2: If } (S(t) < 0.6 * \mathrm{S_{inter}}) && \mathrm{CET} = \beta * \mathrm{PET} * \exp\left(-\frac{0.6*\mathrm{S_{inter}} - S(t)}{S(t)}\right) \\ &\text{Case 3: If } (S(t) < 0) && \mathrm{CET} = 0 \end{aligned} \qquad \text{(Eq. 1)}$$

where $S(t)$ [L] is the actual water level in the soil reservoir, β [-] is a correction coefficient that depends on the type of soil cover. In this study, β has been set equal to 1.

3.2 Management of water flow in the soil reservoir

It has been assumed herein that throughout the hydrological season, the soil water content only varies under the effects of rainfall, evapotranspiration and drainage discharge.

Modeling soil water movement in unsaturated zone to assess water table recharge should cover several complex processes (Milly, 1988; Nielsen et al., 1986; Šimůnek and Bradford, 2008; van Genuchten and Jury, 1987). In the literature, numerous models describing water flow in this zone are available and they use either physical-based or conceptual approach. In this study, we present a conceptual calculation of the water table recharge. Downward water movement through homogenous soil profile is governed mainly by both gravity and matric pressure gradients (ψ) effects. When the soil is dry, the ψ gradients effect is dominating, and when the soil is very wet, gravity effect becomes dominant (Nimmo, 2005). Along the soil profile (extending from the soil surface to the impervious layer under the drains), the soil water content is not uniform and variable with respect to time (Zimmer and Lesaffre, 1989). Indeed, the soil profile can present at the same time dry condition near the soil surface and wet condition at the drain level. Thus, instead of considering this spatial variation, the soil reservoir model depicts the filling of the soil profile and calculates water table recharge as a function of three global thresholds (see Figure 2), i.e.:

1) The minimum soil reservoir level (S_{min}) represents the lower limit of the soil reservoir, below which no water moves in the soil under the effects of either evaporation or root extraction, herein set equal to zero; this reflects the driest soil profile condition.

2) The maximum soil reservoir level (S_{max}) represents the upper limit, at which the total net infiltration recharges the water table gravitationally. In this case, the soil water content lies close to the saturation condition throughout the soil profile. The SD network reaction to a rainfall event is rapid, mainly occurring during the high rainfall events that generate drainage discharge peaks. This subsurface drainage period is referred to as Intense Drainage Season (IDS).

3) Between S_{min} and S_{max}, the reservoir model includes an intermediate threshold (S_{inter}). When the soil reservoir lies between S_{inter} and S_{max}, the soil water content can exhibit a saturation condition close to the drain, while remaining unsaturated at the upper part of the soil profile. In this case, one portion of the infiltrated water contributes to the water table recharge and flows toward drains. The other portion of the infiltrated water continues to fill the soil reservoir. The distribution of net infiltration between water table recharge and soil reservoir filling was conducted by means of partition coefficient α. Thus, the S_{inter} defining the start of the drainage season is used as first soil reservoir parameter. The soil water level difference between S_{inter} and S_{max}, is referred to as the intense drainage season reservoir level (S_{IDS}). As S_{max} variations are dependent on that of S_{inter} (S_{max} must be greater than S_{inter}), S_{IDS} is used as second soil reservoir parameter. The two parameters S_{inter} and S_{IDS} of the conceptual soil reservoir are difficult to estimate from a field measurement; they are mainly determined through model calibration.

The model responsible for managing the behavior of the unsaturated zone is referred to as the water holding capacity (WHC) concept, or RU (acronym for *réserve utile* in French). Consequently, the reservoir model will be referred to hereafter as the "RU" model. The conceptual reservoir ignores the deep infiltration flow, given that such contributions are often negligible during the winter period in hydromorphic soils, due to the presence of clayey layers underneath the drains, which in this study are assumed to be impervious.

In the RU module, water variations in the soil reservoir (ΔS) and water table recharge R(t) at time "t" both depend on the water level in the soil reservoir S(t) at time "t-1". The RU module considers the time variable S(t) and R(t) as uniform between the drain and mid-drain. The calculation algorithm can then be expressed as follows:

- If S(t) lies between S_{min} and S_{inter}: net infiltration increases or decreases the water level in the soil reservoir, depending on its sign (negative or positive), hence: S(t) = S(t-1)+ (P-CET). The

minimum soil reservoir level cannot decrease below zero. During this stage, the water table recharge equals zero.

- If S(t) lies between S_{inter} and S_{max}: when net infiltration is positive, the RU module splits this infiltration into two components via partition parameter α, with the first part (α) recharging the water table and the second part (1-α) continuing to fill the soil reservoir:

$$S(t) = S(t-1) + (1-\alpha) * (P - CET)$$
$$R(t) = \alpha * (P - CET) \quad \text{(Eq. 2)}$$

- If S(t) is equal to S_{max}: when net infiltration is positive, the entire excess infiltration will recharge the water table. Otherwise, when net infiltration is negative, the net infiltration rate will be extracted from the soil reservoir.

3.3 Management of water table flow

In this study, the original SIDRA model is used to simulate water table flow toward drain. The specificity of SD in France is that the drains overlay a clayey layer, assumed herein as impervious. SD flow only occurs when the perched water table rises above the drain, as identified during the intense drainage season. The SIDRA model is only able to simulate drainage discharge during this season. The model does not consider unsaturated flow, by assuming that the net infiltration, calculated as rainfall minus evapotranspiration rate, instantly reaches the water table (Bouarfa and Zimmer, 2000; Lesaffre and Zimmer, 1988; Zimmer et al., 1995).

Water flow toward the drain is influenced by several parameters related to both the SD network geometry (i.e. drain depth and drain spacing) and soil hydrodynamic characteristics. The SIDRA model semi-analytically solves the Boussinesq equation according to the following basic assumptions (Bouarfa and Zimmer, 2000; Lesaffre and Zimmer, 1988):

- The perched water table is a free (unconfined) surface that overlays the impervious horizontal clayey layer. Within the saturated zone, the subsurface flow is assumed to be horizontal, in accordance with Dupuit-Forchheimer (Guyon, 1963; Van Schilfgaarde, 1963);

- The Boussinesq equation is based on the concept of drainable porosity (De Marsily, 1986; Zhang and Zhang, 1986), which serves to relate water table fluctuations to water table recharge. This parameter is also approximated with a “specific yield” or “specific storage” value (Anderson and Woessner, 1992; Rupp and Selker, 2005).

In homogeneous soils, based on these assumptions, a combination of the continuity equation and Darcy's Law leads to the classical 1D nonlinear Boussinesq equation (1904):

$$\mu \frac{\partial \mathrm{h}}{\partial \mathrm{t}} = \frac{\partial}{\partial \mathrm{x}}\left(\mathrm{K_{sat}} h \frac{\partial \mathrm{h}}{\partial \mathrm{x}}\right) + \mathrm{R(t)} \qquad \text{(Eq. 3)}$$

where K_{sat} [LT^{-1}] is the saturated hydraulic conductivity in the horizontal direction, h [L] the water table height above the drain, μ [-] the drainable porosity, R(t) [LT^{-1}] the time-dependent water table recharge, t [T] the time, and x [L] the horizontal position coordinate.

The Boussinesq equation simulates drainage discharge and water table variations assuming that the water table shape remains constant or slightly variable during the steady state or tail recession stages (Guyon, 1963; Van Schilfgaarde, 1963). Modeling of the transient state of a water table depends on the time step adopted (from hourly to daily). For a daily time step, the Boussinesq assumption of a constant water table shape is acceptable, as demonstrated by Tournebize et al. (2004). This assumption allows for a pseudo-separation of variables in both time and space. The spatial integration of the water table shape between drain and mid-drain, using the factor concepts developed by Guyon (1963) and Youngs (1966), results in the following equation solely dependent on the time variable:

$$\mu \mathrm{C} \frac{\mathrm{dH(t)}}{\mathrm{dt}} = -\mathrm{K_{sat}} \frac{\mathrm{H^2}}{\mathrm{L^2}} + \mathrm{R(t)} \qquad \text{(Eq. 4)}$$

where C [-] is defined as the “second water table shape factor”, L [L] the half-drain spacing, and H [L] the water table elevation above the drain at mid-drain. The term $\mathrm{J(H)} = \mathrm{K_{sat}} \frac{\mathrm{H^2}}{\mathrm{L^2}}$ [LT^{-1}] represents an equivalent Hooghoudt equation (Hooghoudt, 1940; Van Der Ploeg et al., 1999) describing the steady-state drainage discharge, in assuming that the drain lies on the impervious horizontal layer. Further

details of different steps establishing the model equations can be found in the publication by Bouarfa and Zimmer (2000).

From Darcy's Law, let's now add the influence of recharge, as established by Lesaffre and Zimmer (1987), which yields the following equation to calculate drainage discharge:

$$Q(t) = AJ(H) + (1 - A)R(t) \quad \text{(Eq. 5)}$$

where A [-] is called the “third water table shape factor”.

The water table shape factors C and A are equal to 0.904 and 0.896, respectively, as calculated by integrating ¼ of the ellipse curve, corresponding to the water table shape between drain and mid-drain (Bouarfa and Zimmer, 2000). Eq. 5 reveals that during the recharge stage, drainage discharge Q(t) is generated by: (i) the water table recession based on the Hooghoudt equation (the A.J(H) term), and (ii) the direct contribution of net recharge (the (1-A).R(t) term). In Eq. 5, the water table shape factor A enables the water table recession to contribute to drainage discharge by a factor of 86.9%, to be subsequently completed with the direct recharge at 13.1% (1-A) of R(t).

In this study, surface runoff is calculated using a simplified approach. Several empirical models are available to calculate surface runoff, such as the model by Horton, and Green and-Ampt (Musy and Higy, 2004). However, most of these models are based on parameters that lack physical meaning and can only be defined by model calibration. The simplest empirical approach consists of assuming that surface runoff occurs when the soil reservoir reaches its maximum storage capacity (Dooge, 1959), i.e. when the soil profile is totally saturated and the water table lies near the soil surface. We thus assume that the generation of surface runoff is independent of the soil infiltration capacity in drained soils. Observations in drained fields do indeed show that the surface runoff rate is reduced, compared to an undrained field, and moreover account for roughly 10% of total outflow, thus confirming the high infiltration capacity of drained soils (Augeard et al., 2005; Kao et al., 1998; Trajanov et al., 2018). In the

SIDRA-RU model, when the water table elevation (H) equals drain depth (d), the excess rainfall is converted into surface runoff.

4 Model evaluation

The aim of this study is to validate the ability new SIDRA-RU model to address the tasks of drainage discharge and drain flow start at the field scale based on the existing experimental observations. We begin by assessing the model performance in order to simulate drainage discharge using the classical calibration and validation criterion KGE (Gupta et al., 2009). Next, we evaluate the model by predicting the drain flow start. A criterion determining the drain flow start dates from both observed and simulated drainage discharge is presented. We finish by conducting an analysis to assess the sensitivity of model parameters with respect to KGE and the drain flow start criteria.

4.1 Model calibration and validation

Running SIDRA-RU requires introducing input data (rainfall and evapotranspiration) as well as field characteristics. The SD geometry data consist of the 0.8-m drain depth (d) and the 5-m half-drain spacing (L). The correction coefficient for the CET calculation, which depends on the type of soil cover (β), equals 1.

The water partition parameter (α) is not considered for model calibration, because its influence on model calibration using observed drainage discharge is negligible (See sensitivity analysis results, section 5.1). During the period when drainage season starts (delimited by S_{inter} and S_{max}), the ratio of drainage discharge to rainfall is typically low. Field observations have indeed shown that during this period, the ratio equals approximately 1/3 (Favrot and Lesaffre, 1984; Lesaffre, 1988; Lesaffre and Morel, 1986). The partition coefficient α is thus set theoretically at 1/3.

The calibration model parameters are: the two soil reservoir parameters (S_{inter} and S_{IDS}), and the two soil hydrodynamic parameters (K_{sat} and μ). This modeling approach assumes uniform hydraulic

properties within the soil profile, thus leading to calibrate an average value of the parameters set for each plot.

A performance assessment of the model must acknowledge the fact that drainage discharge is highly variable during the drainage season. To account for this seasonal variability, the Kling-Gupta efficiency (KGE, Gupta et al., 2009) criterion (Eq. 6) is used for model calibration and validation. This KGE criterion has the advantage of incorporating drainage discharge variability throughout the simulation period by combining the correlation, bias and variability between simulated and observed drainage discharges:

$$\mathrm{KGE} = 1 - \sqrt{(\mathrm{r}-1)^2 + (\varepsilon - 1)^2 + (\Delta - 1)^2} \qquad \text{(Eq. 6)}$$

where Δ denotes the ratio between the mean simulated and mean observed drainage discharges (i.e. the bias), *r* the linear correlation between observations and simulations, and ε the measure of relative variability. KGE values range from -∞ to 1. The model performance is improved when the value of KGE lies close 1 (Gupta et al., 2009).

The limited number of calibration parameters in SIDRA-RU serves to limit the equifinality problem and the possibility of obtaining secondary optima (Coron et al., 2017). The optimization algorithm is based on the drainage discharge results, using the KGE criterion as Objective Function (OF) combined with "airGR" R package (Coron et al., 2017; Michel, 1987). First, a grid-screening algorithm explores the parameters space by systematic examination and extracts the most likely convergence zone (Mathevet, 2005). Second, a steepest - descent local search procedure (Michel, 1991) seeks to improve the OF by refining the previously obtained parameter set. Note that each parameter is independently calibrated without considering their possible correlations. The sampling procedure is based on the probability distribution function (pdf) and the limits of the four calibration parameters (Table 3):

- K_{sat} and μ follow a log-normal distribution (Kosugi, 1999; Ren and Santamarina, 2018; Rousseva et al., 2017; Schaap and van Genuchten, 2006; Suleiman and T. Ritchie, 2001). The pdf and the limits of hydraulic conductivity K_{sat} and drainable porosity μ values in Table 3 were established

from 35 hydrodynamic measurements in different drained hydromorphic soils by means of Guyon's pumping test (Lesaffre, 1990). These experiments were carried out in the 1980's as part of the measurement campaign initiated by the French Ministry of Agriculture that allowed establishing 70 referenced soil areas (Lagacherie, 1987);

- The soil reservoir parameters (S_{inter} and S_{IDS}) follow a normal distribution similar to that used for maximum soil water content (Biswas, 2019; Brocca et al., 2007);

- Table 3: Characteristics of the pdf representing the variations in SIDRA-RU parameters

SIDRA-RU parameters	Pdf type	Limit interval		Mean	Standard deviation
		Min	Max		
S_{IDS} (mm)	Normal	10	55	33.3	17
S_{inter} (mm)	Normal	55	225	138.4	53.3
K (m/day)	Log-normal	0.03	4.63	0.9	3.17
μ (-)	Log-normal	0.015	0.13	0.031	1.926

The model evaluation is performed using the split-sample test (Klemeš, 1986), by dividing the 16 seasons (Table 2) of daily drainage discharge measurements into two equivalent periods: Period P1, from 1994 to 2002, and Period P2, from 2002 to 2010. For each period, the model was run in turn for both calibration and validation of drainage discharge. Figure 3 shows the mean variations in yearly cumulative rainfall and drainage during these two periods on plots T03 and T04. Note that Period P1 is wetter than P2, with a higher variation in the yearly cumulative rainfall and drainage discharge (Figure 3 displays the various box widths). It then becomes interesting to test the behavior of model calibration and validation during these two defined periods.

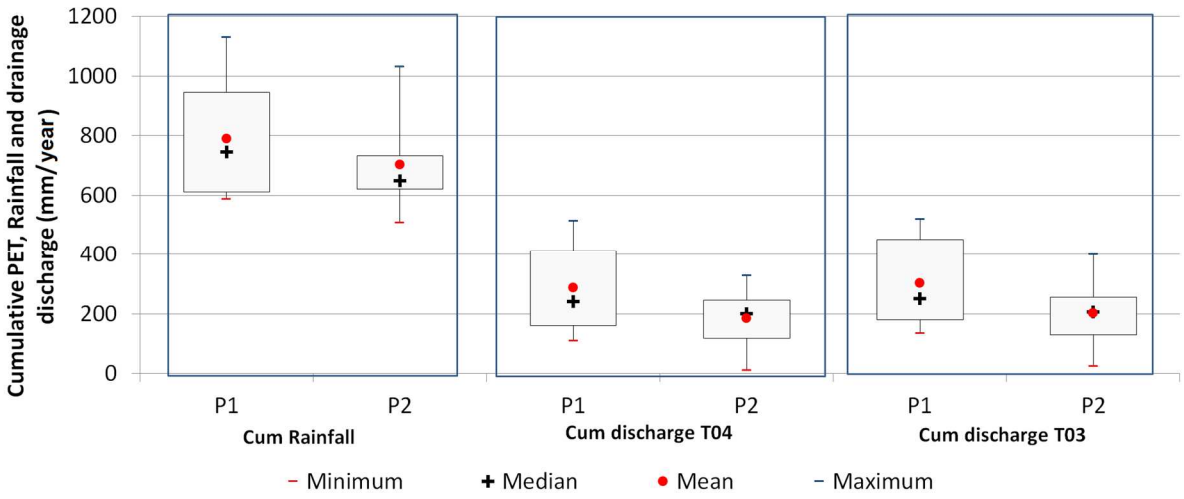

Figure 3: Comparison between periods P1 and P2 - the mean variations in yearly cumulative rainfall and drainage discharge data on plots T03 and T04. The boxes are delimited by the 25% and 75% quartiles.

4.2 Assessment of drain flow start dates

To assess model accuracy in predicting the drain flow start, a criterion has been established in this study, based on the mean of the absolute difference between observed and simulated drain flow start dates (X_{diff}). This criterion is calculated as follows:

$$X_{diff} = \text{mean}\,[\text{abs}\,(Date_{obs} - Date_{sim})] \quad \text{(Eq. 7)}$$

where $Date_{sim}$ and $Date_{obs}$ (in Julian days) are the determined dates of drain flow start from the observed and simulated drainage discharge, respectively, using this dynamic threshold; “abs” represent the absolute value.

The best date prediction occurs when X_{diff} lies near zero. This criterion, in calculating a mean value for the 8 drainage seasons for each period, is sufficient to evaluate model performance in predicting the drain flow start. It is not used however for model calibration.

4.3 Sensitivity analysis of the performance criteria

The objective of the sensitivity analysis is to identify the model input parameters exerting the greatest influence on two performance criteria, namely drainage discharge (using KGE criterion) and the drain flow start criterion (X_{diff}).

Several sensitivity analysis methods are available to analyze model effectiveness (Iooss and Lemaître, 2015; Saltelli, 2008). In light of the low number of input parameters, it is possible to perform a global sensitivity analysis (GSA) of SIDRA-RU using the Sobol method (Sobol, 1993), based on the variance decomposition principle. The purpose of this method is to allocate a fraction of the total variance in the evaluation criterion to each model parameter. The main advantage of this method is its strong performance with nonlinearities that can be often problematic in hydrological modeling (e.g Gatel et al., 2019; Muñoz-Carpena et al., 2007). When considering a model with several parameters, the Sobol method allows quantifying their impact on the model response as well as their interactions regarding the evaluation criterion (Pianosi et al., 2016; Saltelli et al., 2000).

The total variance of the model output, in this case the quality criteria of drainage discharge and X_{diff}, is allocated to each parameter using two sensitivity indices: the first-order sensitivity index (Si), and the total sensitivity index (TSi). The Si index represents the direct impact of each parameter taken alone on total variability, while TSi is defined as the sum of the impact of each parameter taken alone and in interaction with others on total variability. Several methods exist to define the Si and TSi index values, and no single one prevails over the others. Consequently, it is recommended to use several methods to compute the sensitivity indices in order to assess the robustness of GSA. In this study, we tested three variance estimators from (i) Saltelli (2002), named Saltelli2002, (ii) Jansen (1999), named Jansen, and (iii) Martinez (2011), named Martinez. Si has been computed based on the same estimators as TSi, plus the Roalhs estimator (Tissot and Prieur, 2015), named ROALHS.

The SIDRA-RU sensitivity analysis is focused on the following parameters: soil hydraulic conductivity (K_{sat}), drainable porosity (μ), intermediate reservoir level (S_{inter}), the intense drainage season reservoir

459 level (S_{IDS}), and partition coefficient α. The Sobol sampling procedure is based on the probability
460 distribution function (pdf) and the limits defined for all calibration parameters presented in Table 3
461 and the partition coefficient α, which follows a uniform distribution and ranging from 0 to 1.

462 In practice, input parameter was sampled in its respective pdf, as defined in Table 3. The sampling size
463 was *n* = 1,000, and the total number of simulations for Np = 5 parameters was thus: N_{tot} = (Np+2)*n =
464 (5+2)*1,000 = 7,000. Bootstrap methods were then implemented to evaluate the uncertainty
465 associated with each estimator, considering the 95% confidence interval, and 100 bootstrap replicates.

466 5 Results

467 This section reports the results obtained by the SIDRA-RU model in terms of optimal criterion
468 performance. The first subsection will discuss the sensitivity analysis results of the five model
469 parameters (K_{sat}, μ, S_{inter}, S_{IDS} and α) with respect to the drainage discharge (by mean of KGE criterion)
470 and X_{diff} criteria. The second subsection will provide the results obtained for the calibration and
471 validation of four model parameters (K_{sat}, μ, S_{inter} and S_{IDS}) using the daily drainage discharge in the KGE
472 criterion, and analyze the results obtained for yearly cumulative of drainage discharge and surface
473 runoff. Next, the reliability of the model in predicting the drain flow start will be assessed using the
474 X_{diff} criterion. The assumption of approximating the soil WHC by S_{inter} (section 3.1) will be assessed by
475 comparing the S_{inter} values and the measured WHC for both plots T03 and T04 (Table 1).

476 5.1 Sensitivity analysis

477 Drainage discharge simulation T04_P1 (Table 4, section 5.2) has been used as a reference for the
478 sensitivity analysis of the five SIDRA-RU model input parameters (K_{sat}, μ, α, S_{inter}, S_{IDS}). This analysis
479 generated 20 first-order indices (Si) and 15 total-order indices (TSi) per criterion (using drainage
480 discharge and X_{diff}). Figure 4 shows that the various methods used, all present a similar hierarchy of
481 input effects on each criterion, with small deviations, thereby confirming the reliability of the
482 sensitivity analysis conducted. As regards the drainage discharge, hydraulic conductivity (K_{sat}) is the

parameter featuring the highest Si index (from 0.4 to 0.6); it explains nearly half of the total model variance with respect to this criterion. Drainable porosity μ reflects values of the Si index around 0.2. The TSi index exhibits an identical trend; its values for K_{sat} are close to 0.8 and for μ close to 0.5. The last three parameters (α, S_{inter}, S_{IDS}) all display values for both the Si and TSi indices of close to zero and have negligible influence on drainage discharge. Sobol (2002) and Martinez (2011) estimators show a greater difference between Si and TSi for K_{sat} and μ, hence highlighting strong interactions between them. In contrast, the TSi for α, S_{inter} and S_{IDS} parameters lie close to zero, thus indicating that taken alone or interacting with others, these parameters exert no influence on drainage discharge. In considering the very limited effect of parameters α, S_{inter} and S_{IDS}, it can be concluded that the interactions are essentially occurring between K_{sat} and μ, thus demonstrating that these two parameters are the only ones sensitive to the drainage discharge.

As regards the X_{diff} criterion, S_{inter} is the parameter with the highest Si and TSi indices, with values close to 0.8 for both, hence the importance of this parameter in the model defining drain flow start. The TSi and SI index values for S_{IDS} are nearly zero, thus demonstrating that the X_{diff} criterion is insensitive to this parameter taken alone or in interaction with the other model parameters. Parameter α, reflecting values of Si index around 0.1 and TSI index around 0.18, has little impact on the model performance regarding the drains flow start. The hydrodynamic soil parameters K_{sat} and μ exert no influence on the X_{diff} criterion.

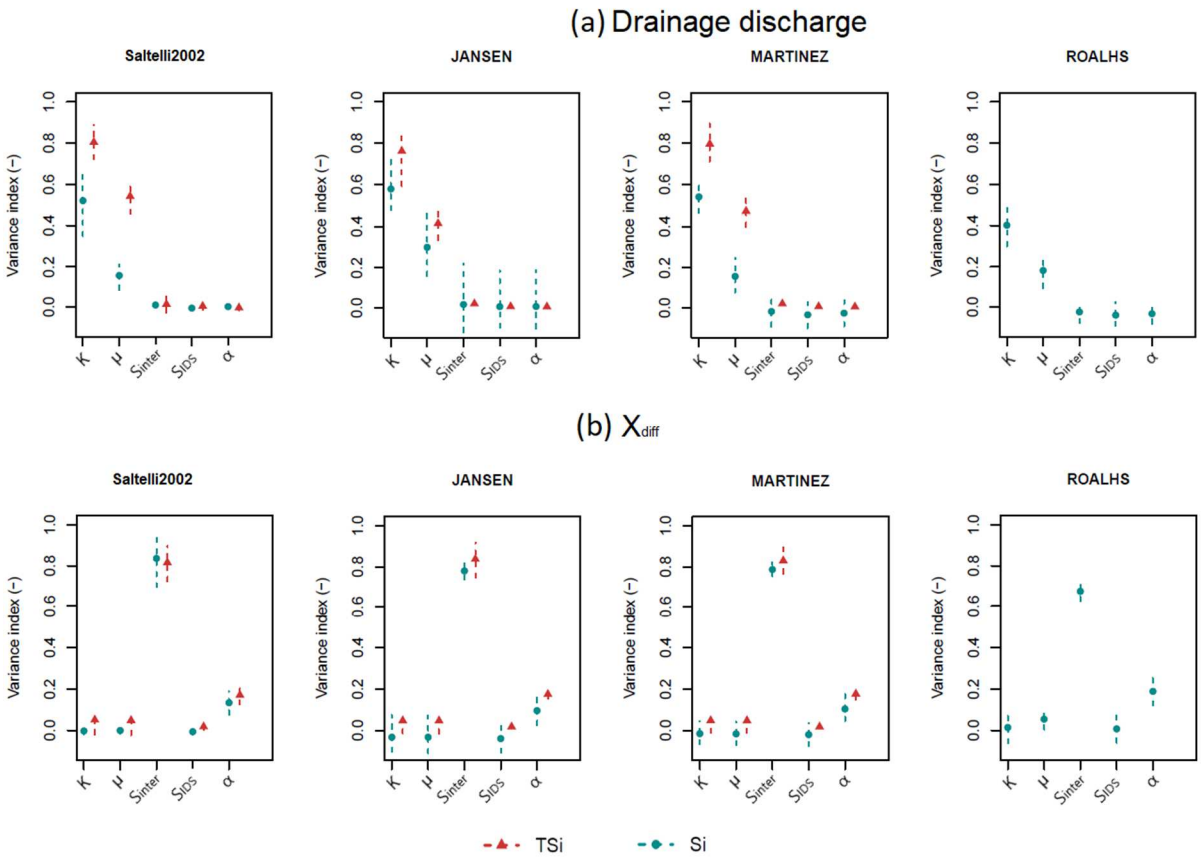

Figure 4: Sensitivity analysis of the five SIDRA-RU model input parameters with respect to both drainage discharge and X_{diff} criteria using the Sobol method with four variance estimators (Saltelli2002, Martinez, Jansen and Roalhs). The blue points represent the first-order Sobol (Si) indices and red points the Total-order Sobol (TSi) indices; dashed lines indicate the uncertainty of each index, considering the 95% confidence interval.

5.2 Model performance assessment

The split-sample test yields calibration and validation results in two parameter sets for each plot (Table 4). Simulations using either period P1 or P2 for calibration are followed by the suffix P1 or P2, for plots T03 and T04, respectively. The KGE values obtained exceed 0.81 for calibration and 0.75 for validation, thus indicating that model calibration can be considered good enough for hydrological modeling (Knoben et al., 2019). However, the calibrated parameters differ slightly depending on the selected calibration period. This variability is mainly influenced by the hydrological variability of period P1, as compared with P2 (Figure 3). For the various calibration tests, the resulting values of drainable porosity

515 μ are identical, while those of hydraulic conductivity K_{sat} range from 0.54 to 0.73 m/day. This difference
516 is more pronounced for the soil reservoir parameters. Note that the calibrated S_{inter} values
517 overestimate the measured WHC, calculated as water held by the soil between the drain and the soil
518 surface (see Table 1). As the WHC has been approximated by S_{inter} (see section 3.1), this result reveals
519 that part of the soil below the drains can contribute to water storage before the start of the drain flow.

520 Table 4: Split-sample test results of model performance based on drainage discharge data
521 from plots T03 and T04

Simulation	**Calibration period P1 (1994-2002)**	**Validation period P2 (2002-2010)**		**Calibrated parameters**			
	KGE	**KGE**	x_{diff} **(days)**	**K_{sat} (m/d)**	**μ (-)**	S_{inter} **(mm)**	S_{max} **(mm)**
T03_P1	0.846	0.751	5.5	0.73	0.05	105.5	110.6
T04_P1	0.818	0.82	8.0	0.71	0.05	119.3	127.1
	Calibration period P2 (2002-2010)	**Validation period P1 (1994-2002)**		**Calibrated parameters**			
T03_P2	0.839	0.78	7.5	0.54	0.05	102.4	130.7
T04_P2	0.871	0.785	6.0	0.73	0.05	140.0	152.9

522

523 The graphical comparison between the measured and simulated drainage discharges of plot T04, using
524 calibration period P1 (simulation T04_P1), is illustrated in Figure 5. The results obtained from plot T03
525 show the same variations as from plot T04, discussed herein. The two graphs, for the calibration and
526 validation steps, indicate that the simulated daily drainage discharge is in good agreement with
527 observed values, during both high and low drainage seasons (Figure 5). This simulation slightly
528 underestimates the observed peak discharge and slightly overestimates the low and medium discharge
529 values. The model does not capture some of the observed peak flows, such as those in July 2001,
530 August 2003 and July 2009, and does not correctly simulate the drain flow start of some drainage
531 seasons, e.g. December 2001. These inaccuracies might be explained by the use of SAFRAN rainfall,

defined on an 8 km × 8 km grid instead of that measured in the field as input data, or else by drainage discharge measurement errors, which are difficult to verify. Aside from these few simulation shortcomings, the model faithfully reproduces the drainage discharge observations.

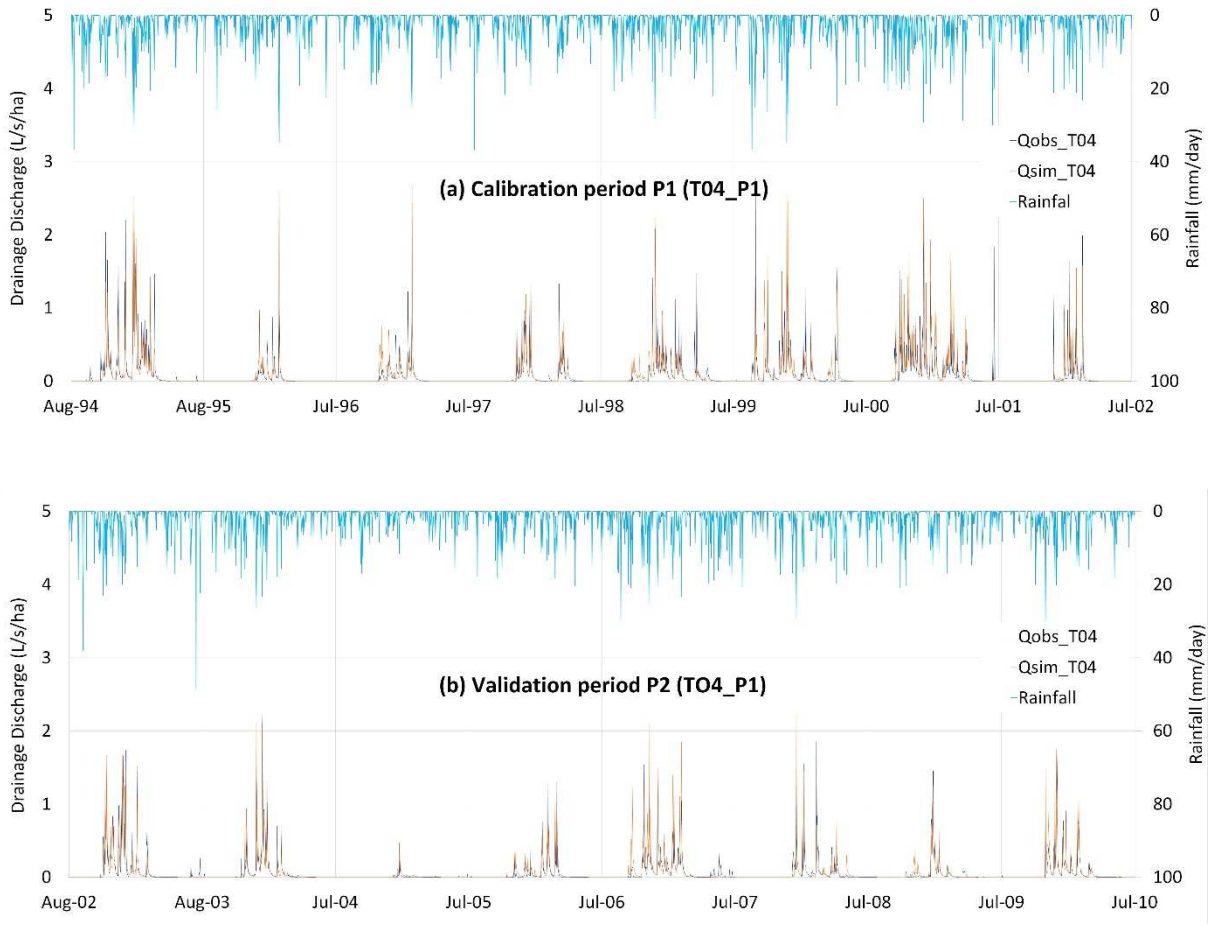

Figure 5: Calibration (period P1) and validation (period P2) of the SIDRA-RU model using observation data from plot T04

For simulation T04_P1, Figure 6 shows the variations in yearly cumulative rainfall, the measured and simulated drainage discharge and surface runoff (mm/season), and the drainage flow start time differential (days). At the scale of a hydrological season, except for a few wet years, the simulated cumulative drainage discharge lies close to the observed values (to within 10%). The mean simulated drainage discharge of 250 mm/season is in good agreement with the observed volume of 236 mm/season (Table 2). The yearly simulation of surface runoff (calculated by the model as excess rainfall) is of the same order of magnitude as the available data observations (from 1995 to 2004).

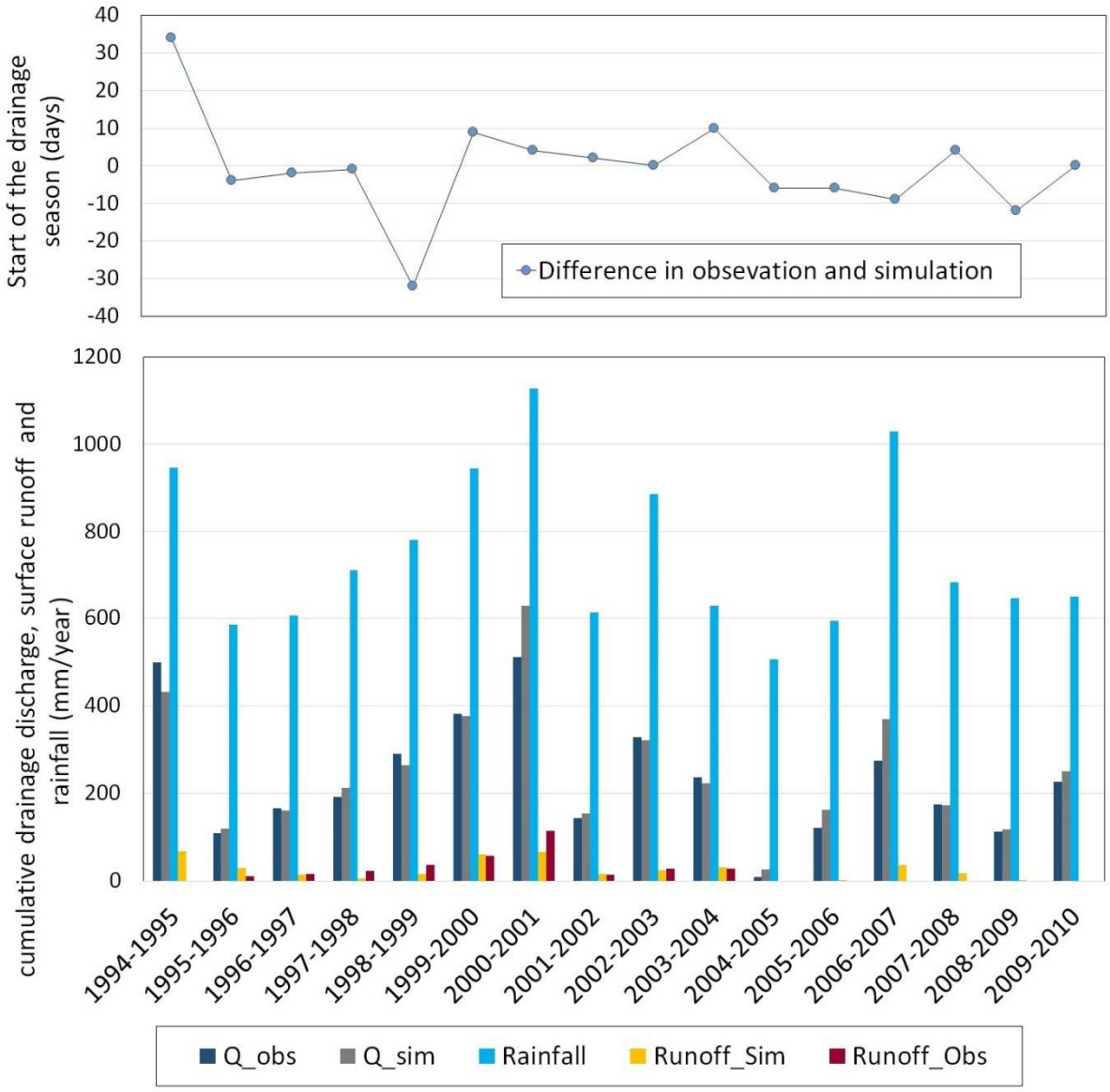

546

547 Figure 6: Comparison between yearly cumulative observation and simulation results for plot T04,
548 using the parameter set of calibration period P1 (T04_P1): rainfall, simulated and observed drainage
549 discharge and surface runoff [mm/year], and the difference in simulated and observed drainage flow
550 start times [days].

551 The reliability of the SIDRA-RU model in predicting drain flow start was also assessed using the X_{diff}
552 criterion (Eq. 7). The median values of X_{diff} are less than 8 days for both plots (Table 4). For simulation
553 T04_P1, Figure 6 shows that the model accurately simulates the drain flow start, except for seasons
554 1994-95 and 1998-99, when the difference in simulated and observed drain flow start times was equal
555 to 34 and -32 days, respectively. For the entire simulation period, the model output a median X_{diff} value

of 5 days with a standard deviation of 10 days. These results demonstrate that model calibration based on the drainage discharge observation does not reduce the large discrepancies between drain flow start observation and simulation.

6 Discussion

The main objective of integrating a soil reservoir module (RU) into the SIDRA model consists of simulating a continuous drainage discharge over several hydrological years, as opposed to the original SIDRA model, which is only applied during the intense drainage season and *a priori* qualified by users. The SIDRA-RU performance analysis has been based on optimizing the four model parameters (K_{sat}, μ, S_{inter}, S_{IDS}) to maximize calibration criterion KGE, based on drainage discharge. The comparison between daily observation and simulation of drainage discharge proves to be satisfactory in most seasons examined. Simulations reveal good flow dynamics, with KGE values greater than 0.75, which are efficient in hydrological modeling (Knoben et al., 2019). The peak flows have been correctly simulated, yet some events have been slightly under-or overestimated. These small deviations might be related to the input data or the model's simplifying hypothesis, e.g. neglecting deep infiltration and preferential flow (Pluer et al., 2020). In terms of yearly cumulative drainage discharge and surface runoff, these results show that the simulations lie very close to the observations. As for the observations themselves (Table 2), the simulated surface runoff is less than 12% of total outflow.

The model evaluation demonstrates that for most drainage seasons, the observed drain flow start times are predicted with good accuracy. However, large gaps can be noticed when predicting the drain flow start times for certain seasons; the main cause may be related to the rainfall regime. Indeed, continuous rainfall does in fact cause a progressive rewetting of the soil profile until formation of the perched water table. Any heavy rainfall on dry soil can generate preferential flow toward the drains before total saturation of the soil profile (Zimmer, 1992). Since this process is neglected in SIDRA-RU, the prediction of drain flow start time gets delayed. Despite such simulation differences, the model is still capable of predicting drain flow start with a relatively acceptable standard deviation of 10 days.

Thus, the model can offer farmers and agricultural operators accurate critical period to avoid the application of pesticides and fertilizers, other than changing or limiting their application to the autumn or winter period (Brown and van Beinum, 2009; Lewan et al., 2009).

The sensitivity analysis of SIDRA-RU parameters, according to the Sobol method, indicates that model performance with respect to the drainage discharge (using KGE Criterion) solely depends on hydrodynamic parameters K_{sat} and μ. The soil reservoir parameter S_{inter}, which describes the threshold when the soil reservoir is capable of recharging the drained water table, has negligible impact on model sensitivity, as regards drainage discharge. Meanwhile, model performance relative to the drain flow start (as described by the X_{diff} criterion) mainly depends on the parameter S_{inter}.

In our modeling approach, the soil hydrodynamic parameters K_{sat} and μ, governing the water table flow, have zero impact on the determination of the drain flow start dates. Indeed, the water table only starts to form when water storage in the soil reservoir lies above the S_{inter} threshold in the RU module (Section 3.2). This module considers the unsaturated zone as a single reservoir system defined by its storage level parameters (S_{inter} and S_{IDS}), with instantaneous input (net infiltration) and output (water table recharge). Thus, the RU module does not take into account dynamic flow in the unsaturated zone (e.g. (Niswonger et al., 2006)) nor any influence of the soil hydrodynamic parameters.

The sensitivity analysis has also shown that model parameter α has a negligible impact on the model performance regarding the drainage discharge, thus confirming the assumption to set this parameter to 1/3, within the limit of the SIDRA-RU model proposed in this study (Section 3.2). However, this parameter has a little influence when defining the drain flow start.

In situ, the soil hydrodynamic parameters (K_{sat}, μ) can be estimated using Guyon's pumping test (Chossat, 1995; Guyon and Lesaffre, 1986; Lesaffre, 1990). However, the field estimation of the soil reservoir parameters (S_{inter} and S_{IDS}) is difficult. Theoretically, their values lie close to the measured WHC of the soil profile, which is available from farming professionals. We would suggest determining these values by means of model calibration based on the drain discharge observations.

7 Conclusion

This study has presented a modeling strategy based on the integration of a new module (RU) in order to manage the behavior of the SIDRA model's soil reservoir. This novel concept allows calculating the recharge of the perched water table. Integration of the RU module makes it possible to simulate the flow of soil water through the drainage system. This model is run with four parameters, serving to control the behavior of both soil water storage and hydrodynamic flow of the perched water table, both of which are determined by means of model calibration.

Application of SIDRA-RU at the “La Jaillière” experimental site has revealed its efficiency in simulating drainage discharge during both wet and dry seasons. Simulation output is in good agreement with the observed daily drainage discharge and yearly cumulative volume in most of the seasons studied; in addition, the model correctly identifies the drain flow start, i.e. accurate to within a median value of 5 days and a standard deviation of 10 days.

The sensitivity analysis conducted for five model parameters (K_{sat}, μ, α, S_{inter}, S_{IDS}) indicates various dependencies on the performance criteria tested. The calibration of drainage discharge is mainly sensitive to hydraulic conductivity and drainable porosity, whereas the determination of drain flow start time is sensitive to the soil reservoir parameter S_{inter}. To reduce simulation uncertainties, it is recommended to calibrate S_{inter} and S_{IDS} independently of the K_{sat}, μ calibration using the observed drainage discharges.

The model's ability to predict drain flow start times with good accuracy allows preventing the transfer of agricultural pollutants into the water surface. Predicting the first drainage flows, using 6-days weather forecasts, allows farmers and agricultural operators to plan for the critical application timing and, hence, reduce the level of pesticide transfer. Moreover, this new model simulates the drained yearly volume with a good level of approximation, thus offering the potential for realistic estimations of the annual transfer of various pollutants of agricultural origin by means of SD systems.

Acknowledgments

The authors would like to thank ARVALIS Agricultural Institute (formerly ITCF) for its support in providing the data acquired by the institute from its experimental site at La Jaillière.

References

AGRESTE, 2010. Agricultural census, Ministry of agriculture, food and forestry, France.

Al Jabri, S.A., Youngs, E.G., 2015. Steady-State Water Tables in Drained Lands Modeled Using the HYDRUS Package and Compared with Theoretical Analyses. Journal of Irrigation and Drainage Engineering, 141(9). DOI:doi:10.1061/(ASCE)IR.1943-4774.0000881

Anderson, M.P., Woessner, W.W., 1992. Applied Groundwater Modeling: Simulation of Flow and Advective Transport

Augeard, B., Kao, C., Chaumont, C., Vauclin, M., 2005. Mechanisms of surface runoff genesis on a subsurface drained soil affected by surface crusting: A field investigation. Physics and Chemistry of the Earth, 30(8-10): 598-610.

Biswas, A., 2019. Joint multifractal analysis for three variables: Characterizing the effect of topography and soil texture on soil water storage. Geoderma, 334: 15-23. DOI:https://doi.org/10.1016/j.geoderma.2018.07.035

Blann, K.L., Anderson, J.L., Sands, G.R., Vondracek, B., 2009. Effects of Agricultural Drainage on Aquatic Ecosystems: A Review. Critical Reviews in Environmental Science and Technology, 39(11): 909-1001. DOI:10.1080/10643380801977966

Boithias, L., Sauvage, S., Srinivasan, R., Leccia, O., Sánchez-Pérez, J.-M., 2014. Application date as a controlling factor of pesticide transfers to surface water during runoff events. CATENA, 119: 97-103. DOI:https://doi.org/10.1016/j.catena.2014.03.013

652 Boivin, A., Šimůnek, J., Schiavon, M., van Genuchten, M.T., 2006. Comparison of Pesticide Transport
653 Processes in Three Tile-Drained Field Soils Using HYDRUS-2D. Vadose Zone J, 5(3): 838-849.
654 DOI:10.2136/vzj2005.0089

655 Bordoloi, R., Das, B., Yam, G., Pandey, P. K., and Tripathi, O. P., 2019. Modeling of Water Holding
656 Capacity Using Readily Available Soil Characteristics. Agricultural Research 8, 347-355.

657 Bouarfa, S., Zimmer, D., 2000. Water-table shapes and drain flow rates in shallow drainage systems.
658 Journal of Hydrology, 235(3-4): 264-275.

659 Boussinesq, J., 1904. Recherches théoriques sur l'écoulement des nappes d'eau infiltrées dans le sol et
660 sur le débit des sources. Journal de Mathématiques Pures et Appliquées, 10: 5-78.

661 Brocca, L., Morbidelli, R., Melone, F., Moramarco, T., 2007. Soil moisture spatial variability in
662 experimental areas of central Italy. Journal of Hydrology, 333(2): 356-373.
663 DOI:https://doi.org/10.1016/j.jhydrol.2006.09.004

664 Brown, C.D., van Beinum, W., 2009. Pesticide transport via sub-surface drains in Europe. Environmental
665 Pollution, 157(12): 3314-3324. DOI:https://doi.org/10.1016/j.envpol.2009.06.029

666 Chossat, J.C., 1995. Qualité des sols : méthode de mesure de la conductivité hydraulique horizontale
667 équivalente et de la porosité de drainage in situ. Méthode de Guyon.Norme NF X 31-504.

668 Coron, L., Thirel, G., Delaigue, O., Perrin, C., Andréassian, V., 2017. The suite of lumped GR hydrological
669 models in an R package. Environmental Modelling & Software, 94: 166 - 171.
670 DOI:https://doi.org/10.1016/j.envsoft.2017.05.002

671 Dairon, R., Dutertre, A., Tournebize, J., Marks-Perreau, J., Carluer, N., 2017. Long-term impact of
672 reduced tillage on water and pesticide flow in a drained context. Environmental Science and
673 Pollution Research, 24(8): 6866-6877. DOI:10.1007/s11356-016-8123-x

674 De Marsily, G., 1986. Quantitative hydrogeology. Academic Press, Inc.,Orlando, FL, 464 pp.

675 Dooge, J.C.I., 1959. A general theory of the unit hydrograph. Journal of Geophysical Research (1896-
676 1977), 64(2): 241-256. DOI:https://doi.org/10.1029/JZ064i002p00241

677 Dusek, J., Vogel, T., 2014. Modeling Subsurface Hillslope Runoff Dominated by Preferential Flow: One-
678 vs. Two-Dimensional Approximation. Vadose Zone J, 13(6). DOI:10.2136/vzj2013.05.0082

679 Favrot, J.C., Lesaffre, B., 1984. Science du sol et drainage agricole, Livre jubilaire du cinquantenaire
680 AFES (Association Française pour l'Etude du Sol) 1934-1984. AFES, Paris, pp. 309-319.

681 Gärdenäs, A.I., Šimůnek, J., Jarvis, N., Van Genuchten, M.T., 2006. Two-dimensional modelling of
682 preferential water flow and pesticide transport from a tile-drained field. Journal of hydrology, 2006
683 v.329 no.3-4(no. 3-4): pp. 647-660. DOI:10.1016/j.jhydrol.2006.03.021

684 Gatel, L. et al., 2019. Global evaluation and sensitivity analysis of a physically based flow and reactive
685 transport model on a laboratory experiment. Environmental Modelling & Software, 113: 73-83.
686 DOI:https://doi.org/10.1016/j.envsoft.2018.12.006

687 Gerke, H.H., Dusek, J., Vogel, T., 2013. Solute Mass Transfer Effects in Two-Dimensional Dual-
688 Permeability Modeling of Bromide Leaching From a Tile-Drained Field. Vadose Zone J, 12(2).
689 DOI:10.2136/vzj2012.0091

690 Gowda, P., Mulla, D., Desmond, E., Ward, A., Moriasi, D., 2012. ADAPT: Model use, calibration and
691 validation. Transactions of the ASABE (American Society of Agricultural and Biological Engineers),
692 55: 1345-1352. DOI:10.13031/2013.42246

693 Gramlich, A., Stoll, S., Stamm, C., Walter, T., Prasuhn, V., 2018. Effects of artificial land drainage on
694 hydrology, nutrient and pesticide fluxes from agricultural fields – A review. Agriculture, Ecosystems
695 & Environment, 266: 84-99. DOI:https://doi.org/10.1016/j.agee.2018.04.005

696 Gupta, H.V., Kling, H., Yilmaz, K.K., Martinez, G.F., 2009. Decomposition of the mean squared error and
697 NSE performance criteria: Implications for improving hydrological modelling. Journal of Hydrology,
698 377(1): 80 - 91. DOI:https://doi.org/10.1016/j.jhydrol.2009.08.003

699 Guyon, G., 1963. Considdrations sur l'hydraulique des nappes de drainage par canalisations
700 souterraines.

701 Guyon, G., Lesaffre, B., 1986. Mesures expérimentales au champ utilisées pour caractériser le
702 fonctionnement hydraulique d'une réseau drainé en sol à pseudo-gley. Zeszyty problemowe
703 postepow nauk rolniczych(132): 187-215.

704 Hansen, S., 1984. Estimation of Potential and Actual Evapotranspiration: Paper presented at the Nordic
705 Hydrological Conference (Nyborg, Denmark, August - 1984). Hydrology Research, 15(4-5): 205-212.
706 DOI:10.2166/nh.1984.0017

707 Henine, H., Nédélec, Y., Ribstein, P., 2014. Coupled modelling of the effect of overpressure on water
708 discharge in a tile drainage system. Journal of Hydrology, 511(0): 39-48.
709 DOI:http://dx.doi.org/10.1016/j.jhydrol.2013.12.016

710 Hooghoudt, S.B., 1940. General consideration of the problem of field drainage by parallel drains,
711 ditches, watercourses, and channels, Bodemkundig Instituut, , Groningen, Netherlands.

712 Iooss, B., Lemaître, P., 2015. A review on global sensitivity analysis methods. In: Meloni, C., Dellino, G.
713 (Eds.), Uncertainty management in Simulation-Optimization of Complex Systems: Algorithms and
714 Applications. Springer.

715 Iooss, B., Veiga, S.D., Alexandre, J., Gilles, P., 2020. sensitivity: Global Sensitivity Analysis of Model
716 Outputs

717 Jacquart, C., Choisnel, E., 1995. Un modèle de bilan hydrique simplifié à deux utilisable en
718 agrométéorologie, Association Météo et Climat, .

719 Jansen, M.J.W., 1999. Analysis of variance designs for model output. Computer Physics
720 Communications, 117(1): 35-43. DOI:10.1016/S0010-4655(98)00154-4

721 Jarvis, N., Larsbo, M., 2012. MACRO (v5.2): Model Use, Calibration, and Validation. Transactions of the
722 ASABE, 55(4): 1413-1423. DOI:https://doi.org/10.13031/2013.42251

723 Kao, C., Nedelec, Y., Zimmer, D., 1998. Surface runoff mechanisms and modeling in subsurface drained
724 fields, 7th international drainage symposium in the 21st century : food production and the
725 environment, Orlando, USA, 8-10 March 1998, pp. 258-266.

726 Kirkham, D., 1949. Flow of ponded water into drain tubes in soil overlying an impervious layer. Eos,
727 Transactions American Geophysical Union, 30(3): 369-385. DOI:10.1029/TR030i003p00369

728 Kjær, J. et al., 2011. Transport modes and pathways of the strongly sorbing pesticides glyphosate and
729 pendimethalin through structured drained soils. Chemosphere, 84(4): 471-9.
730 DOI:10.1016/j.chemosphere.2011.03.029

731 Klemeš, V., 1986. Operational testing of hydrological simulation models. Hydrological sciences journal,
732 1986 v.31 no.1(no. 1): pp. 13-24. DOI:10.1080/02626668609491024

733 Knoben, W., Freer, J., Woods, R., 2019. Technical note: Inherent benchmark or not? Comparing Nash–
734 Sutcliffe and Kling–Gupta efficiency scores. Hydrology and Earth System Sciences, 23: 4323-4331.
735 DOI:10.5194/hess-23-4323-2019

736 Kosugi, K., 1999. General Model for Unsaturated Hydraulic Conductivity for Soils with Lognormal Pore-
737 Size Distribution. Soil Science Society of America Journal, 63(2): 270-277.
738 DOI:10.2136/sssaj1999.03615995006300020003x

739 Kristensen, k.J., Jensen, s.E., 1975. A MODEL FOR ESTIMATING ACTUAL EVAPOTRANSPIRATION FROM
740 POTENTIAL EVAPOTRANSPIRATION. Hydrology Research, 6(3): 170-188.
741 DOI:10.2166/nh.1975.0012

742 Kroes, J.G., Van Dam, J.C., Groenendijk, P., Hendriks, R.F.A., Jacobs, C.M.J., 2008. SWAP version 3.2.
743 Theory description and user manual, Alterra, Wageningen, Netherlands

744 Kronvang, B., Strøm, H.L., Hoffmann, C.C., Laubel, A., Friberg, N., 2004. Subsurface tile drainage loss of
745 modern pesticides: field experiment results. Water science and technology : a journal of the
746 International Association on Water Pollution Research, 49(3): 139-47.

747 L Jones, R. et al., 2000. Processes affecting movement of pesticides to drainage in cracking clay soils.
748 Pesticide Outlook, 11(5): 174-179. DOI:10.1039/B007951K

749 Lagacherie, P., 1987. Synthèse générale sur les études de secteur de référence drainage.

750 Lesaffre, B., 1988. Fonctionnement hydrologique et hydraulique du drainage souterrain des sols
751 temporairement engorgés. Thèse de doctorat Thesis, Université Pierre et Marie Curie, Paris VI, 334
752 pp.

753 Lesaffre, B., 1990. Field measurement of saturated hydraulic conductivity and drainable porosity using
754 Guyon's pumping test. Transactions of the ASAE, 33(1): 173-178.

755 Lesaffre, B., Morel, R., 1986. Use of hydrographs to survey subsurface drainage : networks ageing and
756 hydraulic operating. In: Van Wijk, A.L.M., Wesseling, J. (Eds.), Symposium on agricultural water
757 management, Arnhem, NLD, 18-21 June 1985, pp. 175-189.

758 Lesaffre, B., Zimmer, D., 1987. Modélisation du comportement hydraulique d'un sol drainé : débits de
759 pointe et tarissements. Science du sol, 25(4): 231-246.

760 Lesaffre, B., Zimmer, D., 1988. Subsurface Drainage Peak Flows in Shallow Soil. Journal of Irrigation and
761 Drainage Engineering, 114(3): 387-406.

762 Lewan, E., Kreuger, J., Jarvis, N., 2009. Implications of precipitation patterns and antecedent soil water
763 content for leaching of pesticides from arable land. Agricultural Water Management, 96(11): 1633-
764 1640. DOI:https://doi.org/10.1016/j.agwat.2009.06.006

765 Lindstrom, G., Pers, C., Rosberg, J., Stromqvist, J., Arheimer, B., 2010. Development and testing of the
766 HYPE (Hydrological Predictions for the Environment) water quality model for different spatial
767 scales. Hydrology Research, 41(3-4): 295-319.

768 Martinez, J.-M., 2011. Analyse de sensibilité globale par décomposition de la variance, Journée des
769 GdR Ondes & Mascot Num, Institut Henri Poincaré, Paris.

770 Mehdinejadiani, B., Fathi, P., 2020. Analytical solutions of space fractional Boussinesq equation to
771 simulate water table profiles between two parallel drainpipes under different initial conditions.
772 Agricultural Water Management, 240: 106324. DOI:https://doi.org/10.1016/j.agwat.2020.106324

773 Michel, C., 1987. Hydrologie appliquée aux petits bassins ruraux. Centre national du machinisme
774 agricole du génie rural des eaux et des forêts. Antony, Papier, 429 p. pp.

775 Milly, P. C. D., 1988. Advances in modeling of water in the unsaturated zone. Transport in Porous Media
776 3, 491-514.

777 Moriasi, D.N. et al., 2013. Evaluation of the hooghoudt and kirkham tile drain equations in the soil and
778 water assessment tool to simulate tile flow and nitrate-nitrogen. J Environ Qual, 42(6): 1699-710.
779 DOI:10.2134/jeq2013.01.0018

780 Moriasi, D.N., Rossi, C.G., Arnold, J.G., Tomer, M.D., 2012. Evaluating hydrology of the Soil and Water
781 Assessment Tool (SWAT) with new tile drain equations. Journal of Soil and Water Conservation,
782 67(6): 513-524. DOI:10.2489/jswc.67.6.513

783 Muñoz-Carpena, R., Zajac, Z., Kuo, Y.-M., 2007. Global Sensitivity and Uncertainty Analyses of the
784 Water Quality Model VFSMOD-W. Transactions of the ASABE, 50. DOI:10.13031/2013.23967

785 Musy, A., Higy, C., 2004. Hydrologie 1 : Une science de la nature. Presses Polytechniques et
786 Universitaires Romandes, Lausanne, 314 pp.

787 Nielsen, D. R., Th. Van Genuchten, M., and Biggar, J. W., 1986. Water flow and solute transport
788 processes in the unsaturated zone. Water Resources Research 22, 89S-108S.

789 Niswonger, R.G., Prudic, D.E., Regan, R.S., 2006. Documentation of the Unsaturated-Zone Flow (UZF1)
790 Package for modeling Unsaturated Flow Between the Land Surface and the Water Table with
791 MODFLOW-2005. 6-A19. DOI:10.3133/tm6A19

792 Nimmo, J. R., 2005. Unsaturated Zone Flow Processes. In "Encyclopedia of Hydrological Sciences".

793 Nolan, B.T. et al., 2008. Identification of key climatic factors regulating the transport of pesticides in
794 leaching and to tile drains. Pest Management Science, 64(9): 933-944.
795 DOI:https://doi.org/10.1002/ps.1587

796 Pianosi, F., Beven, K., Freer, J., Hall, J. W., Rougier, J., Stephenson, D. B., and Wagener, T., 2016.
797 Sensitivity analysis of environmental models: A systematic review with practical workflow.
798 Environmental Modelling & Software 79, 214-232.

799 Pluer, W. T., Macrae, M., Buckley, A., and Reid, K., 2020. Contribution of preferential flow to tile
800 drainage varies spatially and temporally. Vadose Zone Journal 19, e20043.

801 Qi, H., and Qi, Z., 2016. Simulating phosphorus loss to subsurface tile drainage flow: a review.
802 Environmental Reviews 25, 150-162.

803 Rawls, W.J., Brakensiek, D.L., 1982. Estimating Soil Water Retention from Soil Properties. Journal of
804 the Irrigation and Drainage Division, 108(2): 166-171. DOI:doi:10.1061/JRCEA4.0001383

805 Ren, X.W., Santamarina, J.C., 2018. The hydraulic conductivity of sediments: A pore size perspective.
806 Engineering Geology, 233: 48-54. DOI:https://doi.org/10.1016/j.enggeo.2017.11.022

807 Rousseva, S. et al., 2017. Chapter Two - Soil Water Characteristics of European SoilTrEC Critical Zone
808 Observatories. In: Banwart, S.A., Sparks, D.L. (Eds.), Advances in Agronomy. Academic Press, pp. 29-
809 72. DOI:https://doi.org/10.1016/bs.agron.2016.10.004

810 Rupp, D.E., Selker, J.S., 2005. Drainage of a horizontal Boussinesq aquifer with a power law hydraulic
811 conductivity profile. Water Resources Research, 41(11). DOI:10.1029/2005wr004241

812 Saltelli, A., 2002. Making best use of model evaluations to compute sensitivity indices. Computer
813 Physics Communications, 145(2): 280 - 297. DOI:https://doi.org/10.1016/S0010-4655(02)00280-1

814 Saltelli, A., 2008. Global sensitivity analysis : the primer. Wiley, Chichester.

815 Saltelli, A., Tarantola, S., and Campolongo, F., 2000. Sensitivity Anaysis as an Ingredient of Modeling.
816 Statist. Sci. 15, 377-395.

817 Schaap, M.G., van Genuchten, M.T., 2006. A Modified Mualem–van Genuchten Formulation for
818 Improved Description of the Hydraulic Conductivity Near Saturation. Vadose Zone J, 5(1): 27-34.
819 DOI:10.2136/vzj2005.0005

820 Shokri, A., Bardsley, W.E., 2016. Development, testing and application of DrainFlow: A fully distributed
821 integrated surface-subsurface flow model for drainage study. Advances in Water Resources, 92:
822 299 - 315. DOI:https://doi.org/10.1016/j.advwatres.2016.04.013

823 Šimůnek, J., and Bradford, S. A., 2008. Vadose Zone Modeling: Introduction and ImportanceAll rights
824 reserved. No part of this periodical may be reproduced or transmitted in any form or by any means,
825 electronic or mechanical, including photocopying, recording, or any information storage and
826 retrieval system, without permission in writing from the publisher. Vadose Zone Journal 7, 581-586.

827 Skaggs, R.W., 1980. Drainmod Reference Report. Methods for Design and Evaluation of Drainage-
828 Water Management Systems for Soils with High Water Tables., United States Department of
829 Agriculture, North Carolina state University, Raleigh, North Carolina.

830 Stillman, J.S., Haws, N.W., Govindaraju, R.S., Suresh C. Rao, P., 2006. A semi-analytical model for
831 transient flow to a subsurface tile drain. Journal of Hydrology, 317(1-2): 49-62.

832 Suleiman, A.A., T. Ritchie, J., 2001. Estimating Saturated Hydraulic Conductivity from Soil Porosity.
833 Transactions of the ASAE, 44(2): 235. DOI:https://doi.org/10.13031/2013.4683

834 Tissot, J.Y., Prieur, C., 2015. A randomized orthogonal array-based procedure for the estimation of first-
835 and second-order Sobol' indices. Journal of Statistical Computation and Simulation, 85(7): 1358-
836 1381. DOI:10.1080/00949655.2014.971799

837 Tournebize, J., Kao, C., Nikolic, N., Zimmer, D., 2004. Adaptation of the STICS model to subsurface
838 drained soils. Agronomie, 24(6-7): 305-313.

839 Trajanov, A. et al., 2015. Estimating Drainage Periods for Agricultural Fields from Measured Data: Data-
840 Mining Methodology and a Case Study (La JailliÈRe, France). Irrigation and Drainage, 64(5): 703-
841 716. DOI:https://doi.org/10.1002/ird.1933

842 Trajanov, A. et al., 2018. Modeling the risk of water pollution by pesticides from imbalanced data.
843 Environmental science and pollution research international, 25(19): 18781-18792.
844 DOI:10.1007/s11356-018-2099-7

845 Van Der Ploeg, R.R., Horton, R., Kirkham, D., 1999. Steady Flow to Drains and Wells. In: Skaggs, R.W.,
846 Schilfgaarde, J.V. (Eds.), Agricultural Drainage. Agronomy. American Society of Agronomy, Inc. Crop
847 Science Society of America, Inc. Soil Science Society of America, Inc., Madison, Wisconsin, USA, pp.
848 213-263.

849 Van Schilfgaarde, J., 1963. Design of Tile Drainage for Falling Water Tables Journal of the Irrigation and
850 Drainage Division, 89(2): 1-12.

851 Vidal, J.-P., Martin, E., Franchistéguy, L., Baillon, M., Soubeyroux, J.-M., 2010. A 50-year high-resolution
852 atmospheric reanalysis over France with the Safran system. International Journal of Climatology,
853 30(11): 1627-1644. DOI:10.1002/joc.2003

854 Vincent, B., 2020. TPrincipes techniques et chiffres du drainage agricole De la tuyautique à l'hydro-
855 diplomatie. Sciences Eaux & Territoires(32): 8-15. DOI:10.14758/set-revue.2020.2.02

856 Van Genuchten, M. T., and Jury, W. A., 1987. Progress in unsaturated flow and transport modeling.
857 Reviews of Geophysics 25, 135-140.

858 Willkommen, S., Pfannerstill, M., Ulrich, U., Guse, B., Fohrer, N., 2019. How weather conditions and
859 physico-chemical properties control the leaching of flufenacet, diflufenican, and pendimethalin in
860 a tile-drained landscape. Agriculture, Ecosystems & Environment, 278: 107-116.

Wilson, G.L. et al., 2020. Effects of fertilizer timing and variable rate N on nitrate–N losses from a tile drained corn-soybean rotation simulated using DRAINMOD-NII. Precision Agriculture, 21(2): 311-323. DOI:10.1007/s11119-019-09668-4

Youngs, E.G., 1966. Horizontal seepage through unconfined aquifers with non-uniform hydraulic conductivity. Journal of Hydrology, 4(C): 91-97.

Youngs, E. G., 1980. The analysis of groundwater seepage in heterogeneous aquifers / Analyse de l'infiltration des eaux souterraines dans les aquifères hétérogènes. Hydrological Sciences Bulletin 25, 155-165.

Zhang, W., Zhang, Y., 1986. Methods for Estimating the Drainable Porosity in Nonsteady Drainage Formulas. Hydraulic Design in Water Resources Engineering: Land Drainage. Springer Berlin Heidelberg, Berlin, Heidelberg, pp. 373-382.

Zimmer, D., 1992. Drainage flow patterns and modeling in a seasonally waterlogged heavy clay soil, 6th international drainage symposium "Drainage and water table control", Nashville, USA, 13-15 December 1992, pp. 80-87.

Zimmer, D., Lesaffre, B., 1989. Subsurface drainage flow patterns and soil types, ASAE-CSAE International Summer Meeting, Québec, CAN, 25-28 June 1989, pp. 17.

Zimmer, D., Lorre, E., Lesaffre, B., 1995. Parameter sensitivity and field evaluation of SIDRA model. Irrigation and Drainage Systems, 9(3): 279-296.